

An aerial photograph of a mountain valley. The foreground shows a steep, rocky slope. In the middle ground, a wide river flows through a valley floor, with a small settlement and a large, rectangular, dark-colored field or reservoir. The background is dominated by high, rugged mountains under a clear blue sky.

Aperture synthesis radar imaging in coherent scatter radars: Lesson from Jicamarca

J. L. Chau¹, D. L. Hysell², and M. Urco¹

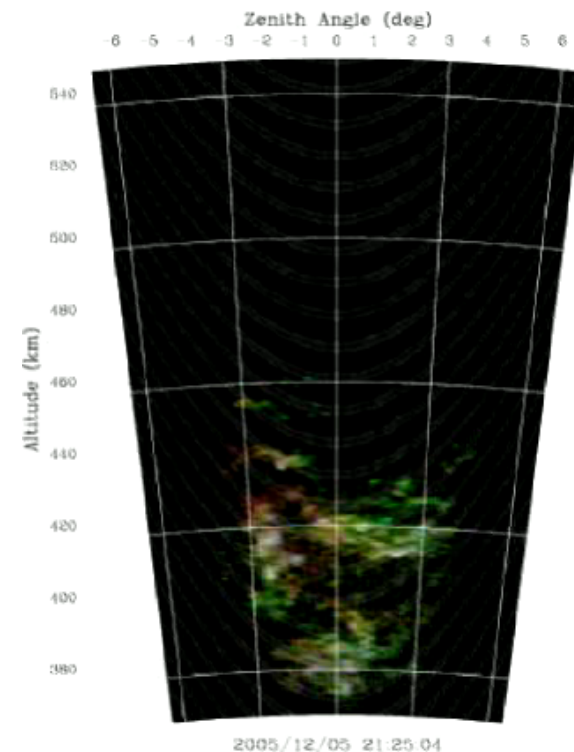
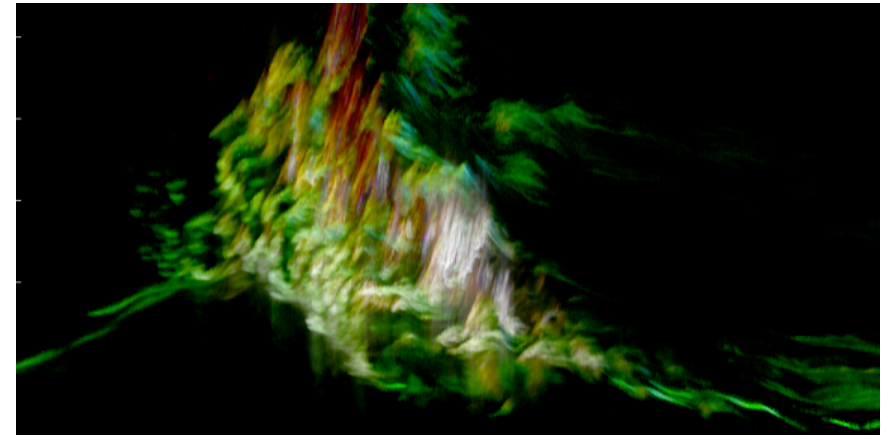
¹Radio Observatorio Jicamarca, Instituto Geofísico del Perú, Lima

²Earth and Atmospheric Sciences, Cornell University, Ithaca, NY, USA

EISCAT Radar School, Sodankyla, Finland, August 29, 2012

Outline

- Introduction
 - Equatorial Ionospheric Irregularities
 - RTI Maps and Slit Camera
- Aperture synthesis for Ionospheric applications
 - Methods
 - Phase calibration
- Jicamarca Examples (EEJ, ESF, 150 km)
- Irregularity comparison: in-situ vs. Radar
- Latest developments

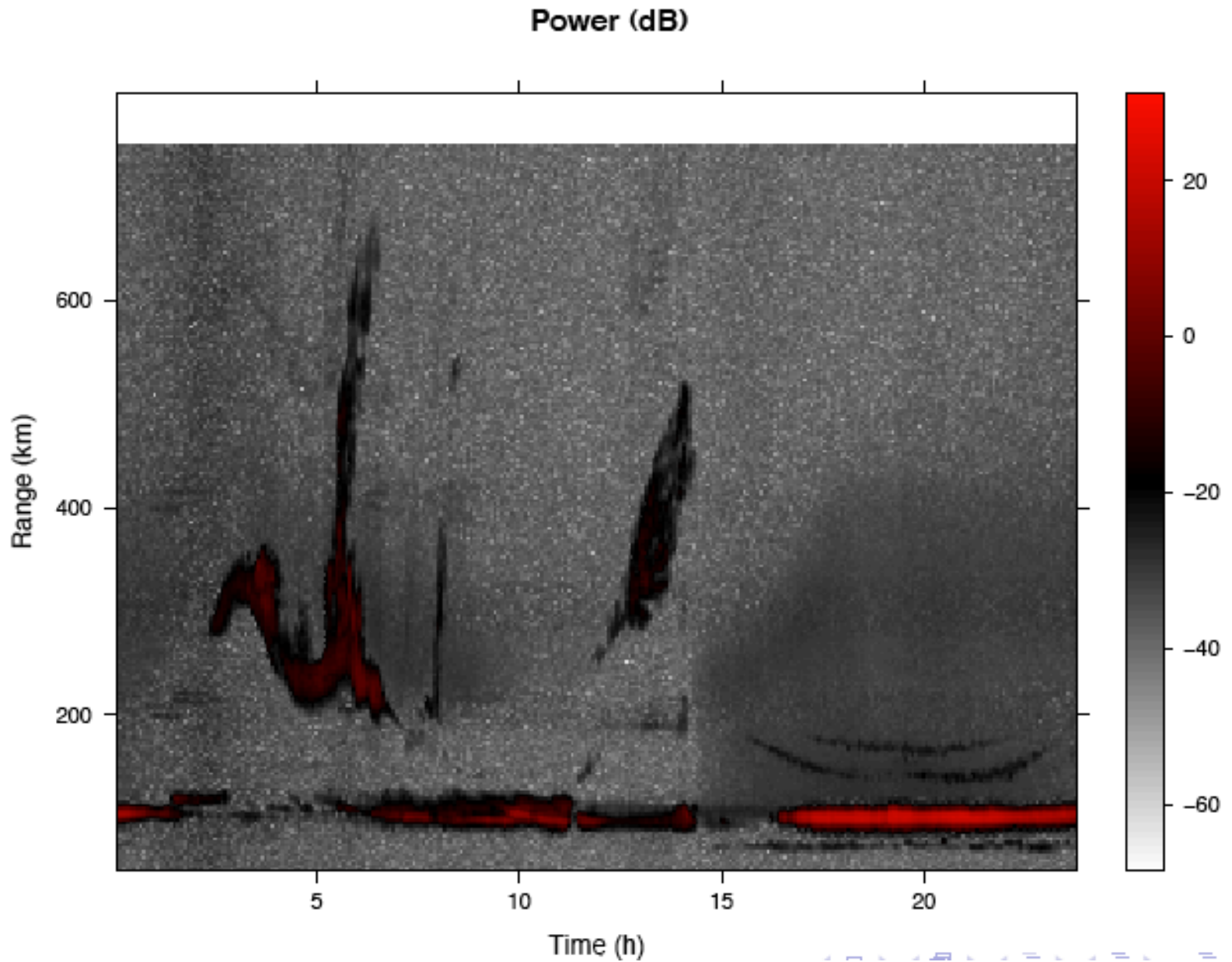


What can we get from single beam radar measurements?



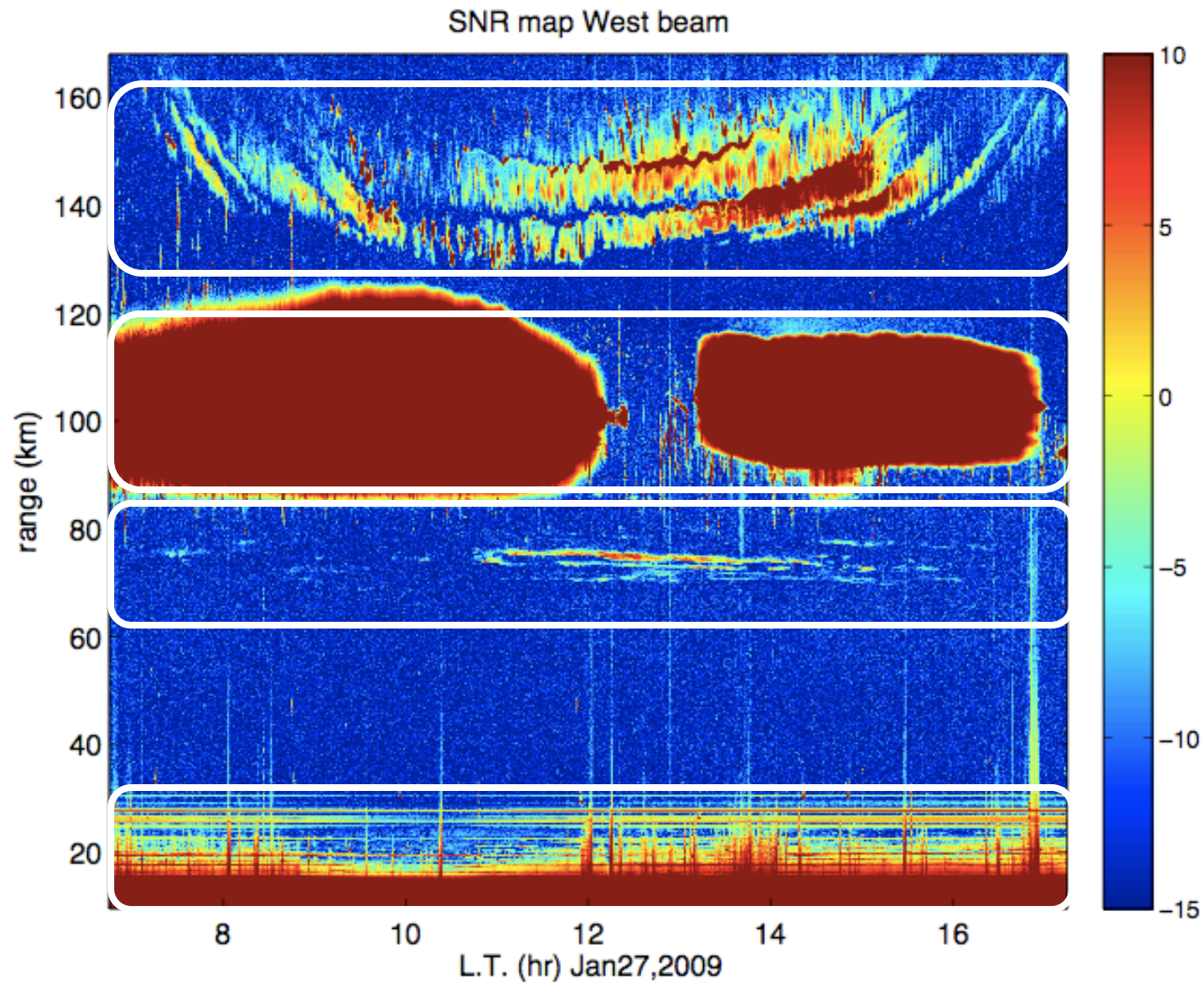
- If the **scattering is volume-filling**, i.e., the whole illuminated volume presents the same statistical characteristics (space and time), then the **information is contained in the spectrum**. For example, in incoherent scatter spectrum, the spectra shape determines the temperature of ions and electrons, and also composition.
- If the scattering is **not volume filling** (the case for most **coherent** echoes), then the single beam information provides a weighted average information inside the illuminated volume. **Is it possible to get spatial information?**
- Note: Coherent echoes are **20-60 dB stronger** than typical ISR echoes.

Equatorial Ionospheric Irregularities

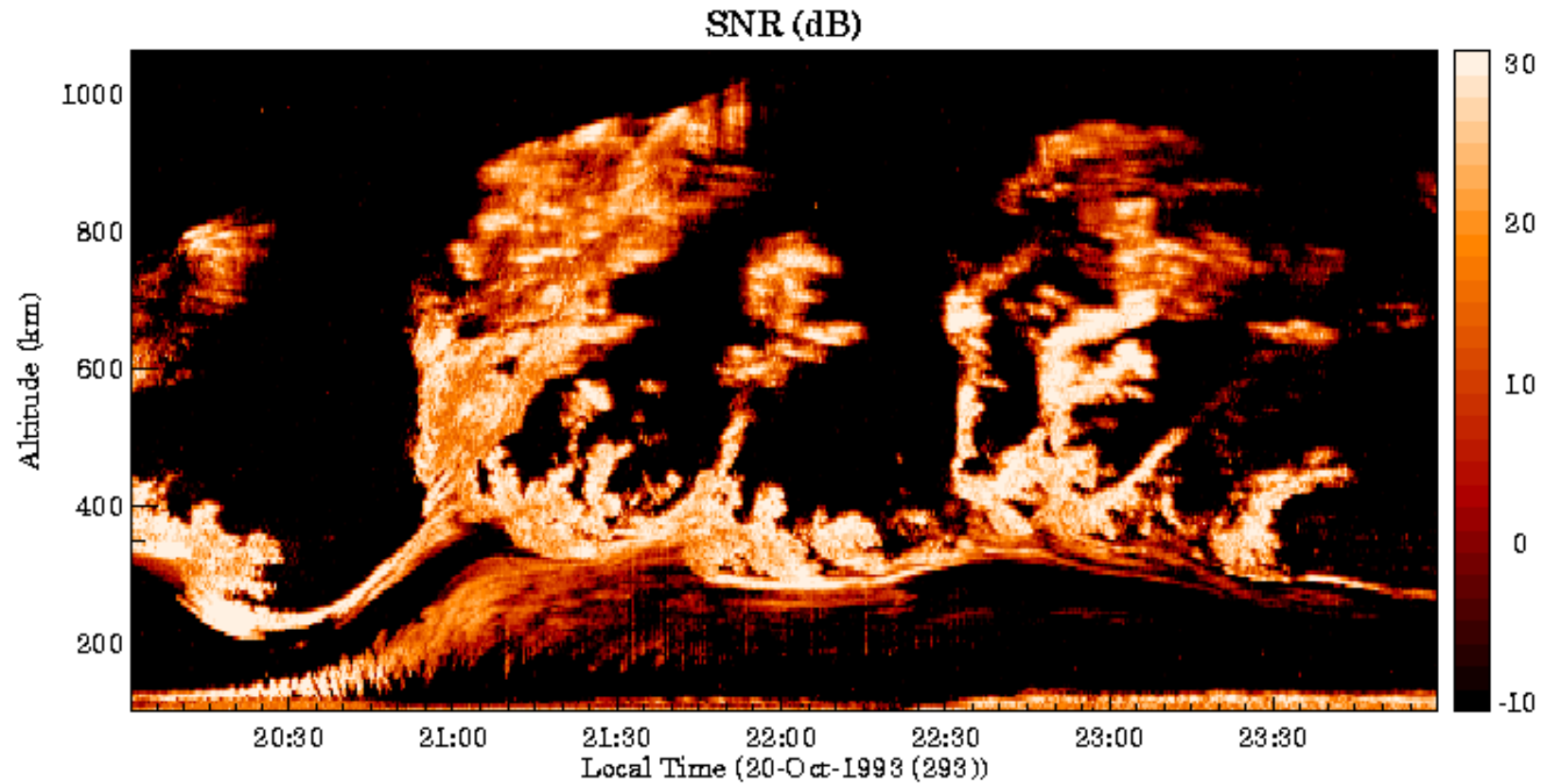


[courtesy of J. Vierinen]

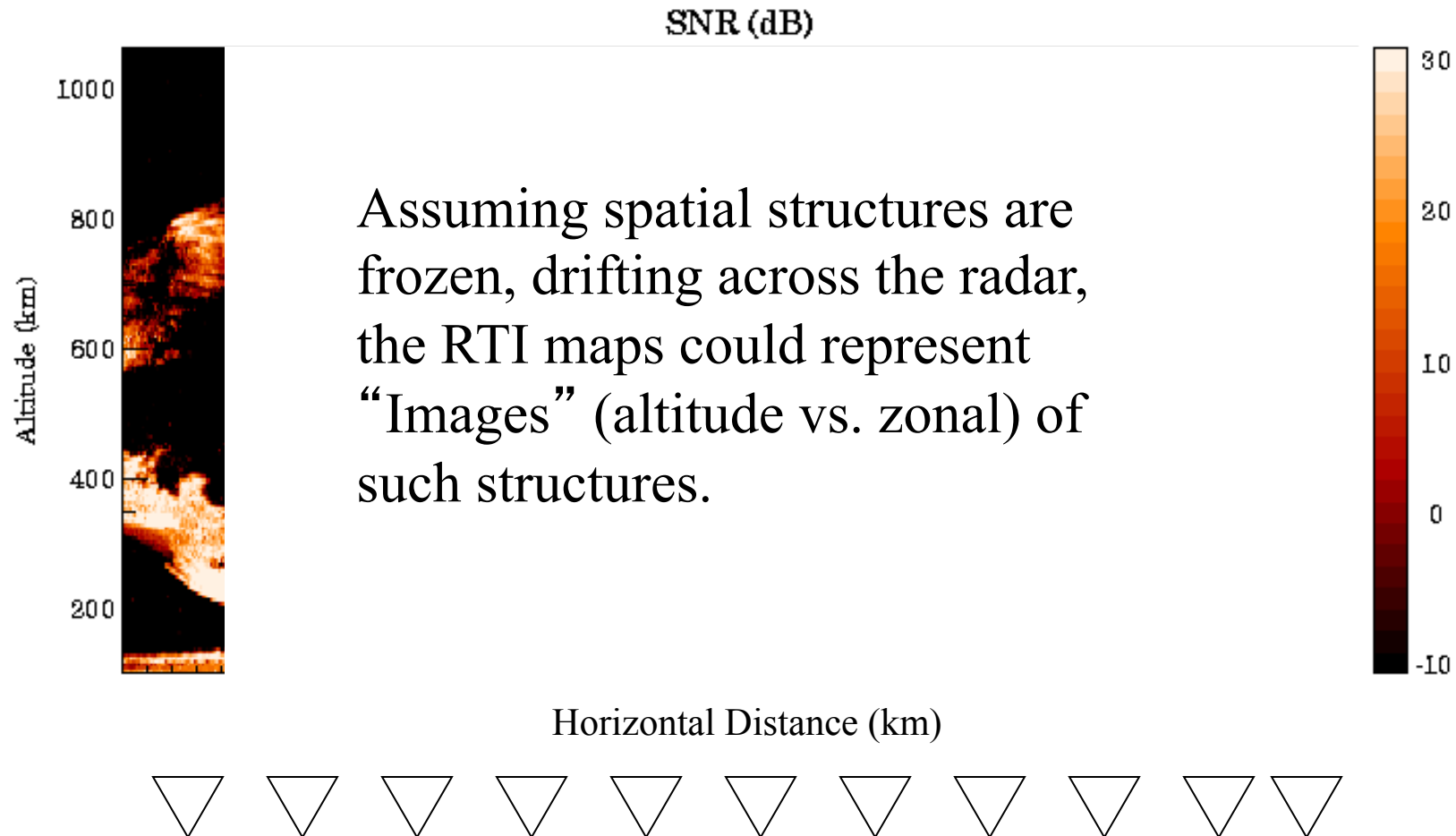
Equatorial Irregularities (2) Below 200 km



Range-Time Intensity (RTI) maps



Range-Time Intensity plots as “Images”: Slit camera interpretation



Slit-camera Analogy and Problems



used with permission ©Tom Dahlin

- In some applications like races it is useful
- In many other applications it provides misleading results:
 - Slow structures are stretch out
 - Fast-moving structures are compressed.
 - In general, it is difficult to discriminate space-time features.

Ionospheric Radar Imaging: Introduction



- The radar imaging techniques used in studying the ionosphere, are an extension of more general techniques used in getting images with non-visible wavelengths (radio frequency, infrared, ultrasound, etc.) and in particular of imaging techniques with radars.
- Among radar imaging techniques we have:
 - SAR Imaging
 - Planetary imaging
 - Underground imaging (Georadar)
 - Meteorological radar images
 - **Ionospheric images**
- Radar imaging are part of more general techniques used in Astronomy.



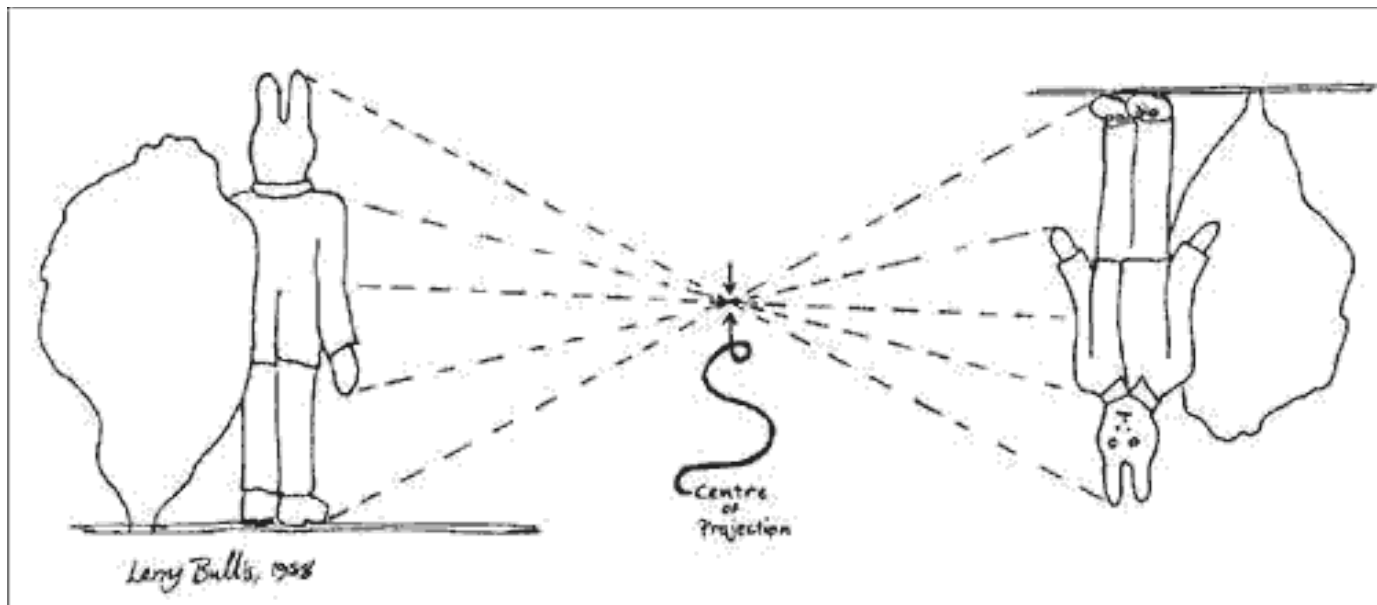
Atmospheric/Ionospheric Target



- In atmospheric applications, besides the problems of discriminating space-time features of moving structures across the beam, **radar have finite beam widths** and “irregularities” can **appear, grow, dissipate, disappear**, inside the beam!

Analogy with an Optical Camera (1)

The pin-hole camera



Object Aperture Image

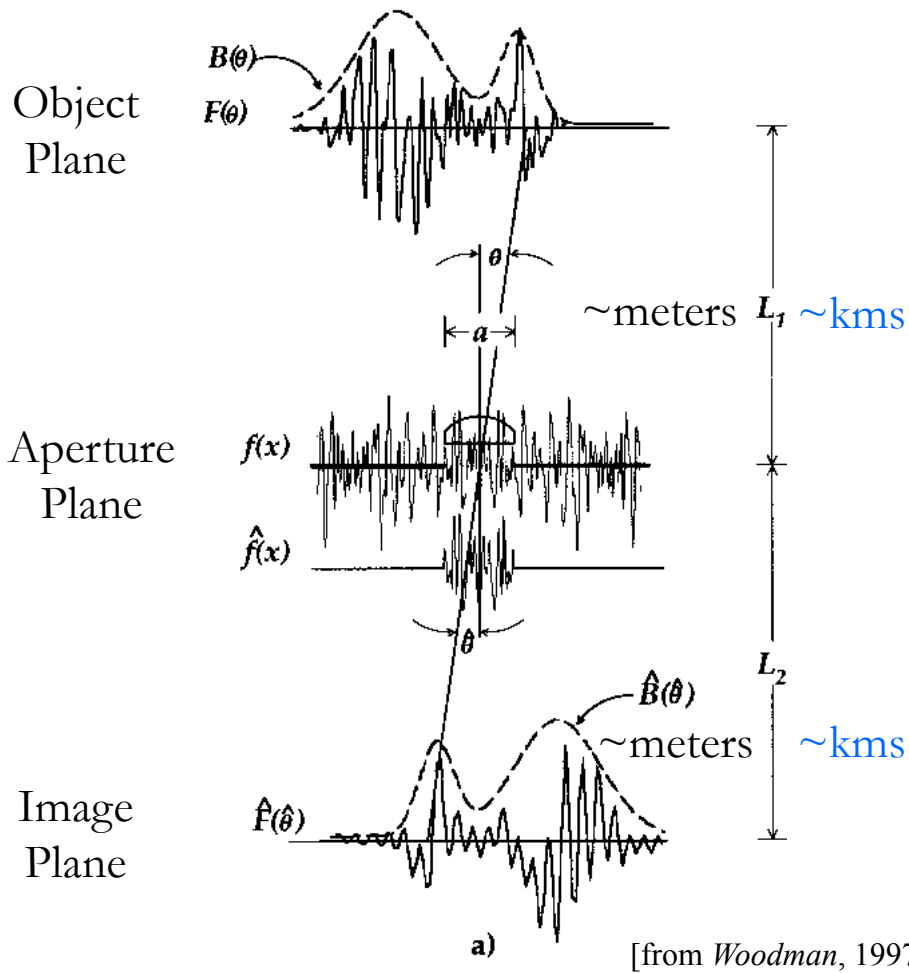
 └──────────┘ └──────────┘

 Far field Far field

Optical wavelength \sim 500 nm

Analogy with an Optical Camera (2)

Fourier Operations



$B(\theta)$ True
Brightness

$$B(\theta) \xleftrightarrow{\text{Fourier}} V(r)$$

$$\hat{B}(\theta) = A^2(\theta) * B(\theta)$$

$$\hat{B}(\theta) \xleftrightarrow{\text{Fourier}} \hat{V}(r)$$

$\hat{B}(\theta)$ Estimated
Brightness

- In **radio astronomy**: Camera without “flash”
- In **radar imaging**: Camera with “flash”

Aperture Synthesis Radar Problem



Given:

$$\hat{V} = \mathbf{a} * \mathbf{a}^* \times \mathbf{M} \mathbf{B}$$

- find \hat{B} that best agrees with B .
- where \mathbf{a} can be an arbitrary complex vector, e.g.,
 - Truncation (like windowing in spectral analysis)
 - Gaps
 - Focusing (needed for near-field applications)

Aperture Synthesis Radar Imaging Algorithms



- **Beamforming or Non-parametric Methods.** These methods do not make any assumption on the covariance structure of the data.
 - Fourier-based
 - Capon or Linear Constraint Minimum variance beam forming
- **Parametric methods.** These methods usually make use of a known functional form B , error covariances, or other *a priori* information.
 - **Maximum Entropy**
 - Model fitting. For example, a Brightness modeled by N anisotropic Gaussian blobs
 - Single value decomposition (SVD)+Multiple Signal Classification (MUSIC) (developed for the localization of discrete scatterers)
- **Other**
 - CLEAN, RELAX (Super CLEAN) (from Radio Astronomy)
 - APES, variants of Capon, etc. (from high resolution spectral analysis)

Ionospheric Radar Imaging: Peculiarities of the target

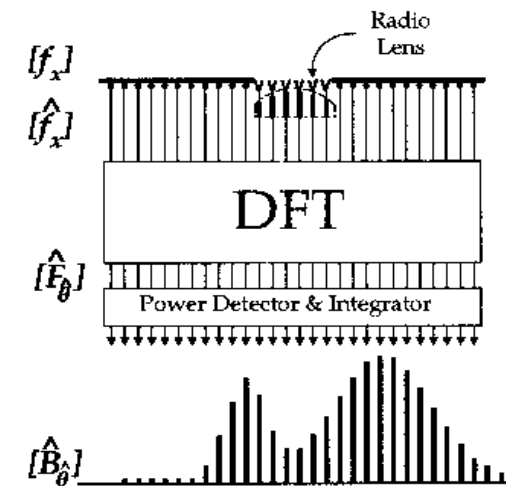
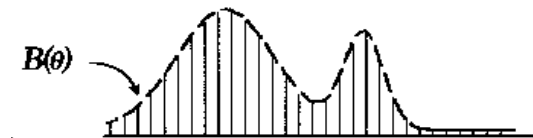


- Spatially **3D**.
- Changes with time in **two different time scales**:
 - short, that defines the “**color**” (frequency spectrum)
 - long, **non-stationary scale**.
- It is **non stationary and non homogeneous**, representing a stochastic process of 4 dimensions.
- Normally, once has a **small number of independent samples to average**.
- Given these characteristics, how do we solve the problem?
 - Shall we do a **simple Fourier inversion**?
 - Are there any **constraints or a priori information** that we could consider? If so, how?

Fourier-based Methods

$$\hat{\mathbf{V}} = \mathbf{a} * \mathbf{a}^* \times \mathbf{MB}$$

- Ideally \mathbf{B} could be obtained by a simple Fourier inversion.
- If \mathbf{a} only represents truncation, i.e., \mathbf{V} is not zero outside the aperture, the estimation can be improved by using proper weighting functions (equivalent to windowing in spectral analysis). The use of weighting functions is also called as *apodization*.
- If \mathbf{a} represents near field effects, e.g., for lower atmospheric applications, the image can be *focused* by correcting it with a known \mathbf{a} .
- If \mathbf{a} is more complicated, which is usually the case (e.g., representing gaps, truncation), clever approaches are needed to “CLEAN/deconvolve” dirty brightness images obtained from Fourier inverting.



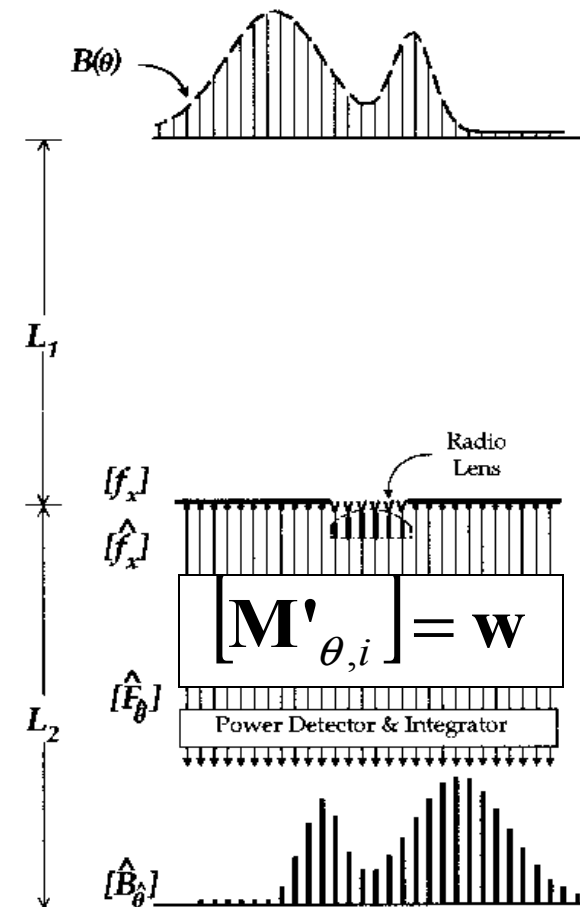
Capon Method

$$\hat{B}_{\text{capon}}(\theta, \omega) = \mathbf{w}^+ \hat{\mathbf{V}}(\omega) \mathbf{w}$$

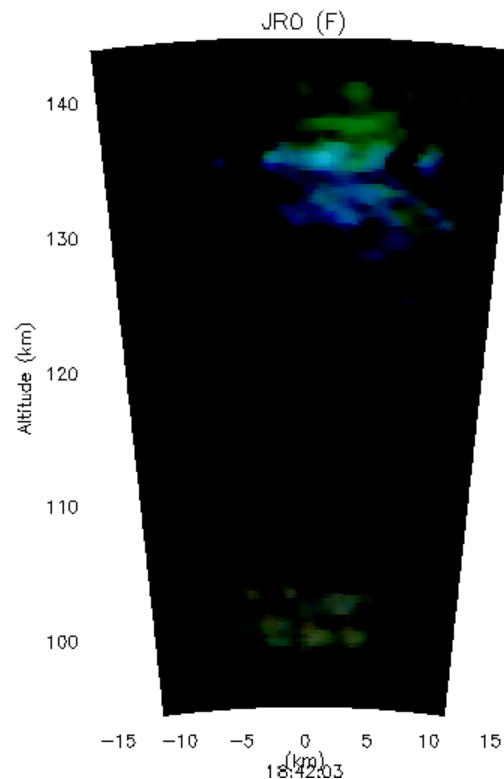
$w(\theta)$ is such that $\hat{B}_{\text{capon}}(\theta, \omega)$ is a minimum under the constrain $\sum w_i(\theta) \text{plane}(\theta, i) = 1$

$$\hat{B}_{\text{capon}}(\theta, \omega) = \frac{1}{\mathbf{e}^+ \hat{\mathbf{V}}(\omega)^{-1} \mathbf{e}}$$

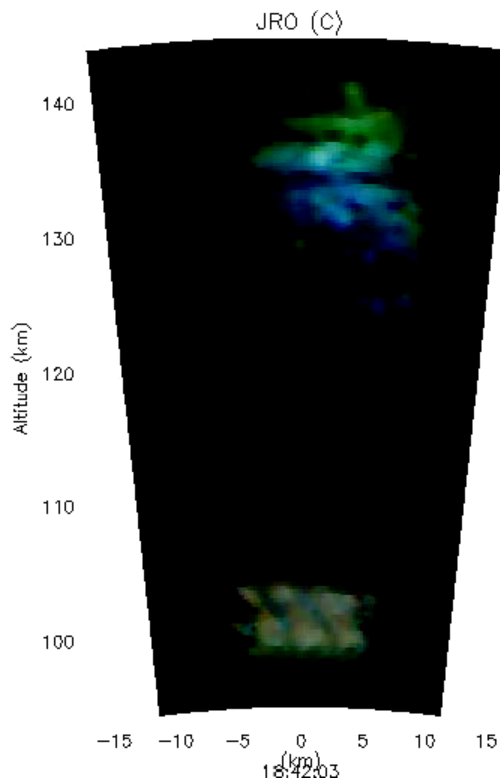
- It reduces to a matrix inversion!!!!
- It is an adaptive method that finds a suitable w , based on the data for each *pointing angle*.



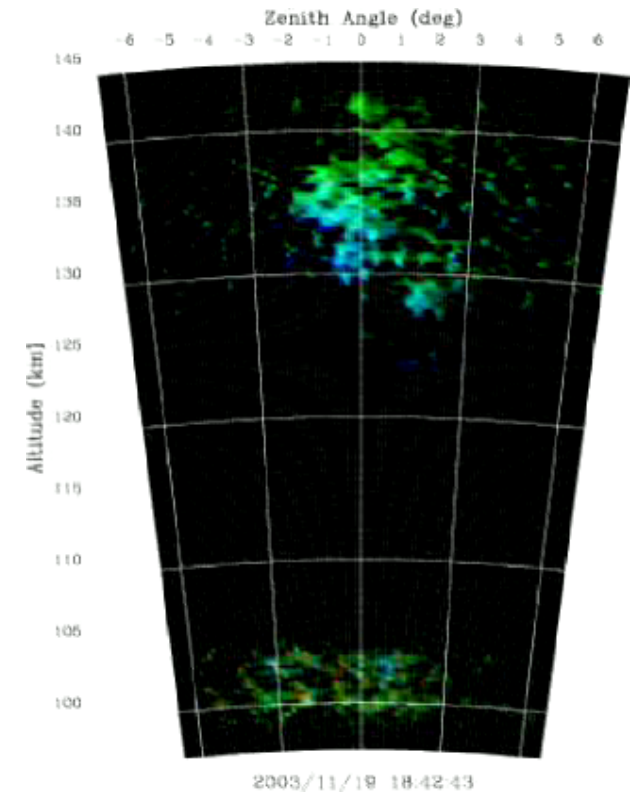
Comparison of Aperture Synthesis Radar Imaging Techniques



- Very Easy to implement
- Very fast processing
- Poor resolution.
- Requires good SNR.
- Usually gets “dirty” images
- Fourier Transform



- Easy to implement
- Fast processing
- Adaptive pointing
- Requires good SNR
- Matrix inversion



- Hard to implement
- Slow processing
- Better estimates and Higher resolution.
- Takes into account statistical errors
- Set of non-linear equations

Maximum Entropy Method (MaxEnt)

- Model-based inversion process where $B(\theta, \omega)$ is a positive definite function constrained to be consistent with the data ($\hat{V}(\mathbf{r}, \omega)$) to a specified accuracy (based on self and statistical errors).

$$\hat{B}(\theta, \omega) \propto \frac{e^{-\lambda_j h_j(\theta)}}{\int e^{-\lambda_j h_j(\theta)} d\theta}$$

λ_j : Lagrange multiplier, one for each visibility measurement

$h_j(\theta)$: point-spread function of the interferometer

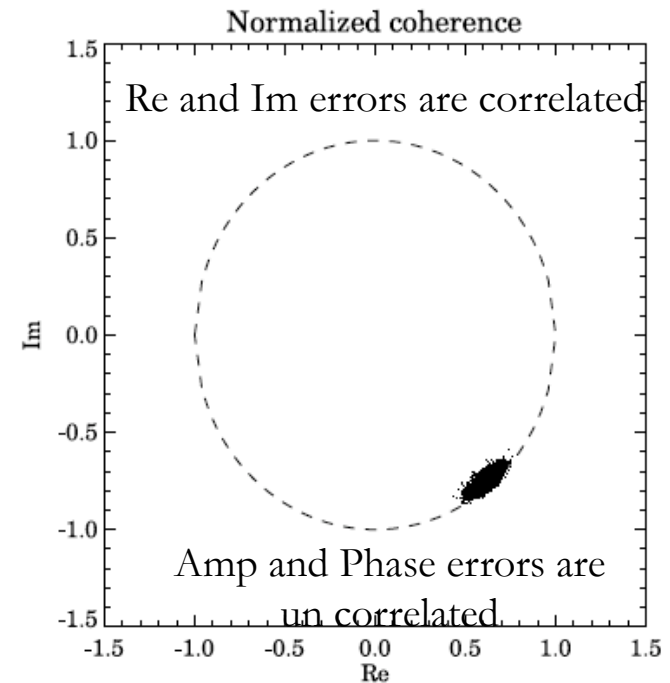
denominator: like the Gibbs canonical partition function

- By maximizing the Shannon Entropy ($S \propto B_j \log B_j$), including the constraints, one gets a well-posed set of **N simultaneous non-linear equations for N Lagrange multipliers**.
- The estimation problem is reduced to solve numerically the set of non-linear equations (e.g., **Powell method**).
- It is a method that “**deconvolves**” via regularization.

MaxEnt: Improvements

- Use of a priori information,
 - Transmitting beam pattern (avoids estimating the image in a region that is not illuminated)
 - Different receiver beam patterns (allows the use of different receiver antenna sizes).
- Full-covariance matrix. Errors between Re and Im components and between baselines are no longer assumed to be uncorrelated.
 - Data and model need to be diagonalized.

$$\delta^2 = \frac{1}{m} \left(\frac{S+N}{S} \right)^2 \left[\begin{aligned} &\rho_{13}\rho_{24}^* \\ &- \frac{1}{2} \left(\frac{S+N}{S} \right) \rho_{34}^* (\rho_{13}\rho_{23}^* + \rho_{14}\rho_{24}^*) \\ &- \frac{1}{2} \left(\frac{S+N}{S} \right) \rho_{12} (\rho_{13}\rho_{14}^* + \rho_{23}\rho_{24}^*) \\ &+ \frac{1}{4} \left(\frac{S+N}{S} \right)^2 \rho_{12}\rho_{34}^* (|\rho_{13}|^2 + |\rho_{14}|^2 \\ &+ |\rho_{23}|^2 + |\rho_{24}|^2) \end{aligned} \right]$$



[from *Hysell and Chau, 2006*]

Model Fitting



- In this technique one makes a parametric model of \mathbf{B} and uses imaging equations to calculate the expected measurements. One then adjust the parameters of the model to get the “best fit” model.
- There are three steps involve in model fitting: (1) design a model defined by a number of adjustable parameters; (2) Choose a *figure-of-merit* function; (3) Adjust the parameters to *minimize the merit function*.
- The goals are to obtain: (1) Best-fit values for the parameters, (2) A measure of the goodness-of-fit of the optimized model (relative to the measurement errors); (3) Estimates of the uncertainty in the best-fit parameters.
- Model fitting has many desirable properties. It can take into account all the details of the measurement process (e.g., antenna patterns, calibration phases), which won't be a simple Fourier transform; and because it operates in the domain of observation (\mathbf{V}), where the statistics of the measurement process are well understood (error covariances), it can estimate the statistical uncertainties of the parameters of the best-fit model, which may be the atmospheric/ionospheric important quantities.
- However, it also has serious problems: it may be difficult to choose a suitable parameterization model, the solutions are not unique, and it can be much, much slower than the conventional beamforming and deconvolution methods.

Uses and practical considerations of model fitting

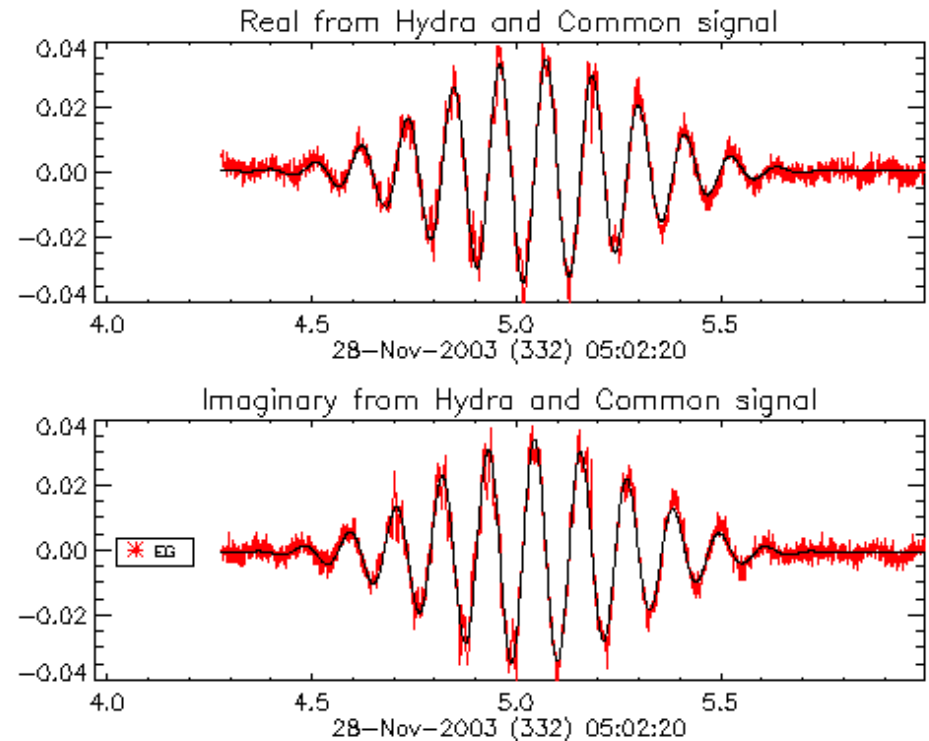


- If the primary objective is the image, then model fitting is not useful, it is better to use conventional methods. However, model fitting is very useful for interpreting sparse or uncalibrated data, and for quantitative analysis.
- Model fitting could be used for the following:
 - Checking and adjusting amplitude and/or phase calibration against known sources, e.g., modeling a Radio Star as a point-source.
 - If the source is simple enough to be accurately represented by a parametric model, then model fitting provides accurate estimates of the model parameters. Estimates derived in this way directly from \mathbf{V} will always be more reliable than parameters estimated from a deconvolved image.
 - Model fitting can be used to improve the behavior of commonly used imaging techniques, e.g., CLEAN and Maxim Entropy.
 - Hybrid methods. For example, one can get an image using conventional images, and improve the estimate using model fitting. The conventional image would serve to provide a very good initial guess and more importantly a good idea of the model to be used, e.g., number of Gaussian blobs.
- Common fitting problems: (1) Finding global minimum; (2) Slow convergence; (3) Constraints; (4) Choosing the right number of parameters or components.

Phase Calibration Procedures

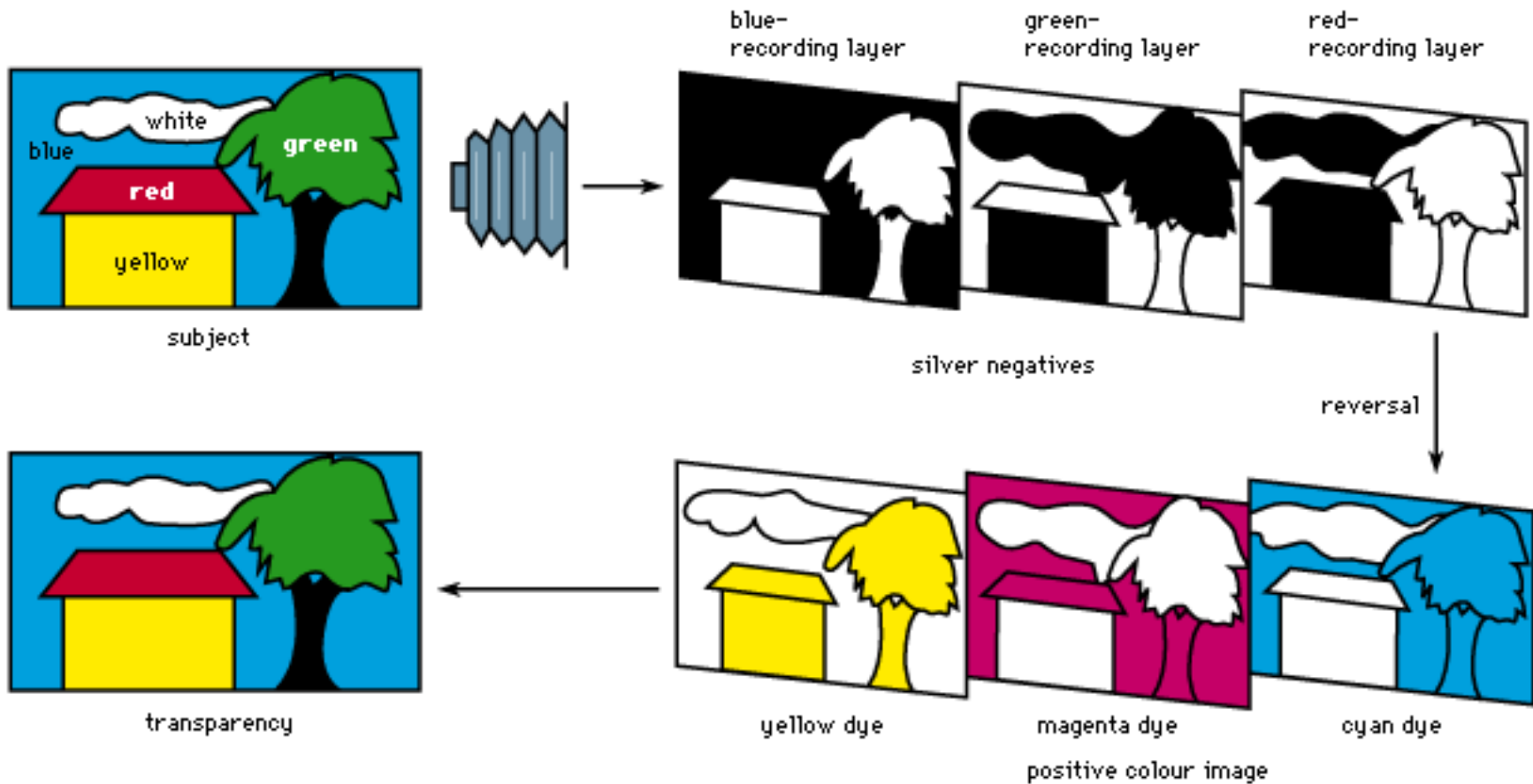


- Use of common signal
 - From natural sources.
 - Radio Stars [e.g., Cygnus A, Hydra]
 - Equatorial electrojet
 - Atmospheric signal after a “long” integration.
 - Meteor head echoes
 - From artificial sources
 - Mobile beacons with a GPS system
 - A common signal fed to receiving lines [e.g., *Kudeki and Sürücü, 1991*].
- “Optimizing” the estimated image
 - Maximize the entropy
 - Minimize peaks

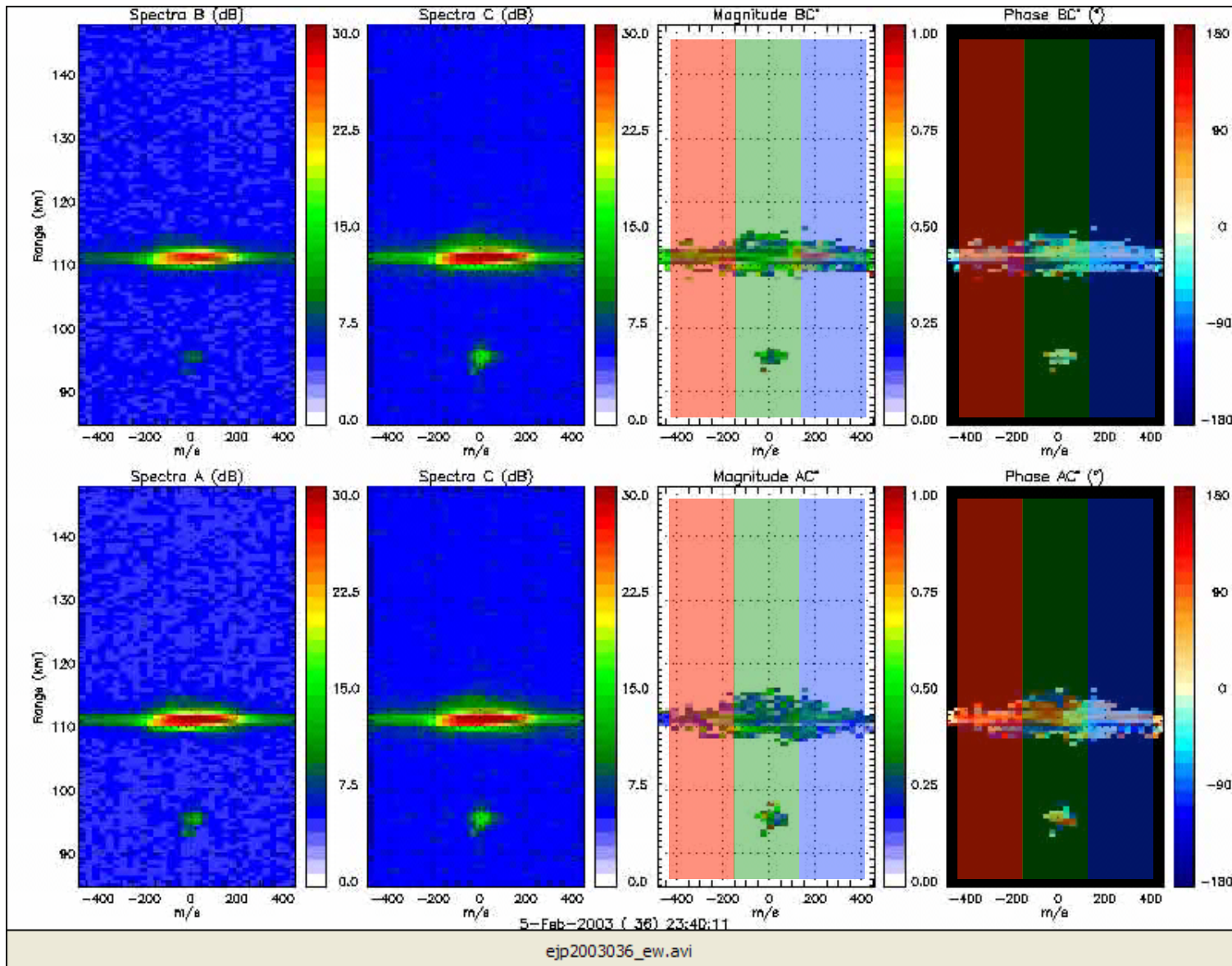


$$\rho_H(t)_{ij} = A(0)_{ij} P_i^{1/2}(\theta_x, \theta_y) P_j^{1/2}(\theta_x, \theta_y) e^{i \frac{2\pi}{\lambda} (dx_{ij} \theta_x + dy_{ij} \theta_y) + iA(1)_{ij}} + A(2)_{ij} + iA(3)_{ij}$$

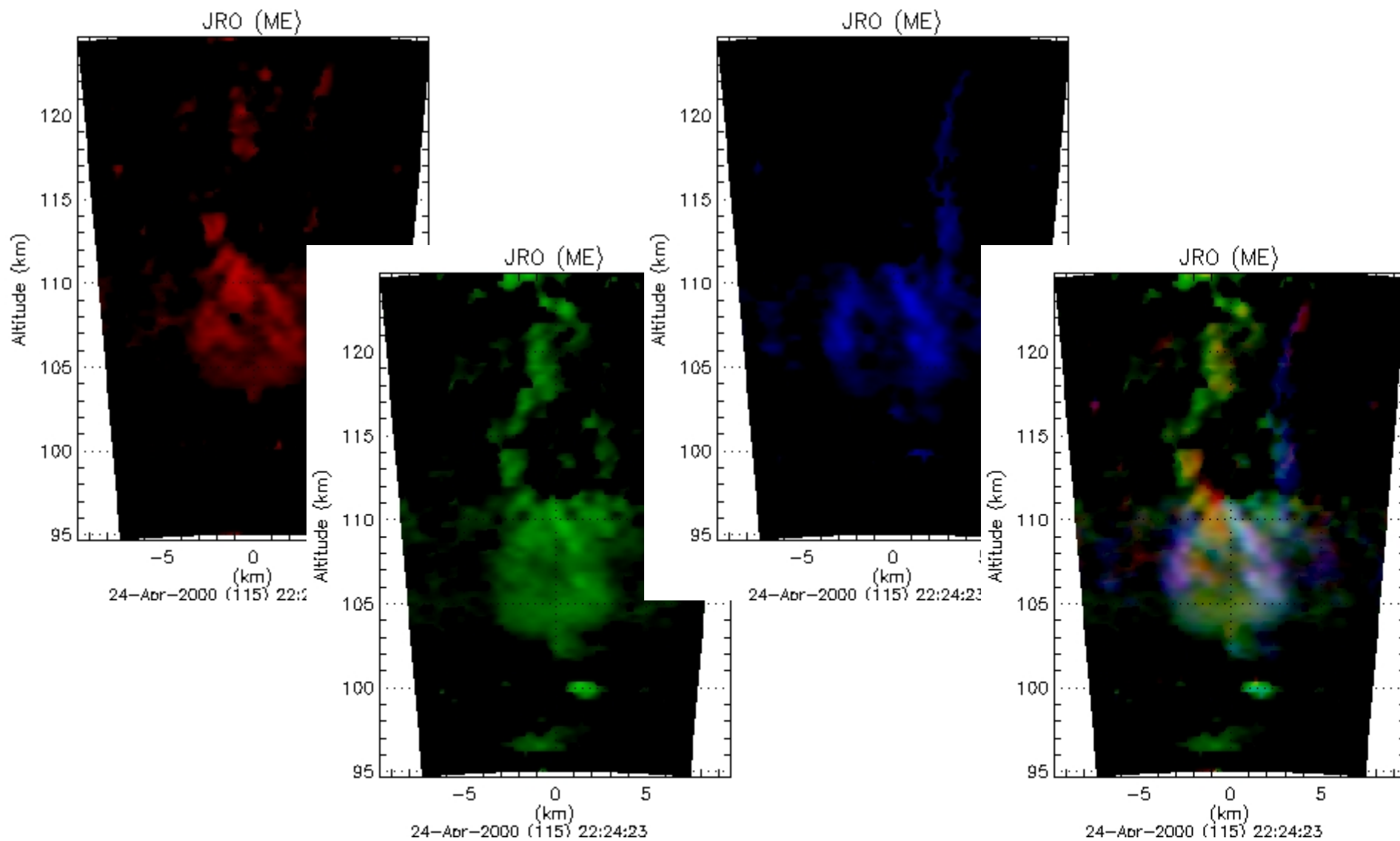
How to display radar images (1)



How to display radar images (2)



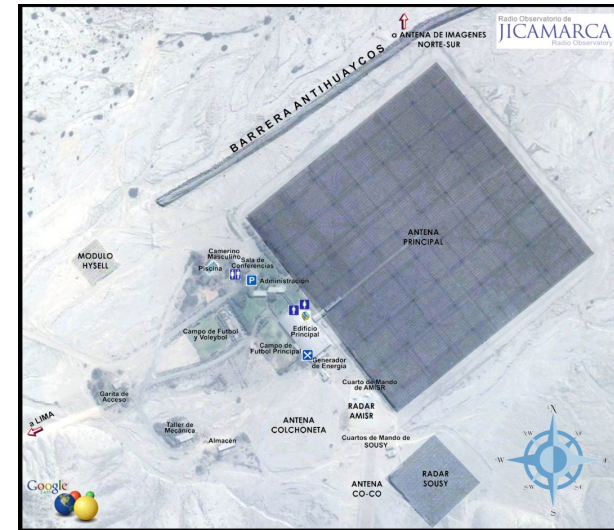
How to display radar images (3)



The Jicamarca Radio Observatory



- Built in 1961 by the US NBS and then donated to IGP in 1969.
- Operating frequency: 50 MHz
- Antenna type: array of 18,432 dipoles, organized in 8x8 cross-polarized modules.
- Pointing directions: within 3 degrees from on-axis. Phase changes are currently done manually.
- Transmitters: 3 x 1.5 MW peak-power with 5% duty cycle.
- Located “under” the magnetic equator (dip 1°).



Examples of ESF Radar Imaging at Jicamarca

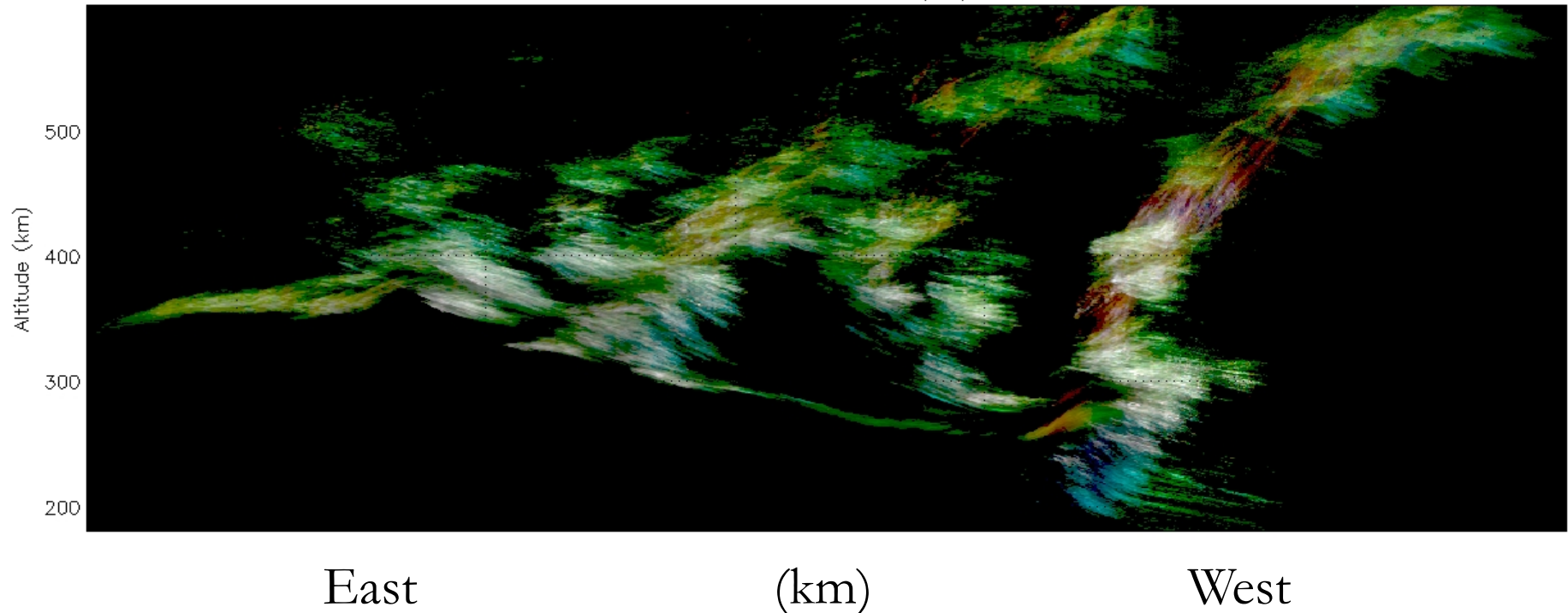


- Tx using two quarter antennas, phased to have a **wide beam** in the EW direction.
- **8 digital Rx** channels for “imaging”. A pair of modules can be used for single baseline interferometry.
- **Automated phase calibration procedure**, using beacon on the hill (relative). Absolute calibration from Hydra, meteor-heads, ...
- **16-32 “colors”** (FFT points)
- ESF images are obtained every 2 seconds and 300 m. The **angular resolution is $\sim 0.1-0.2^\circ$**



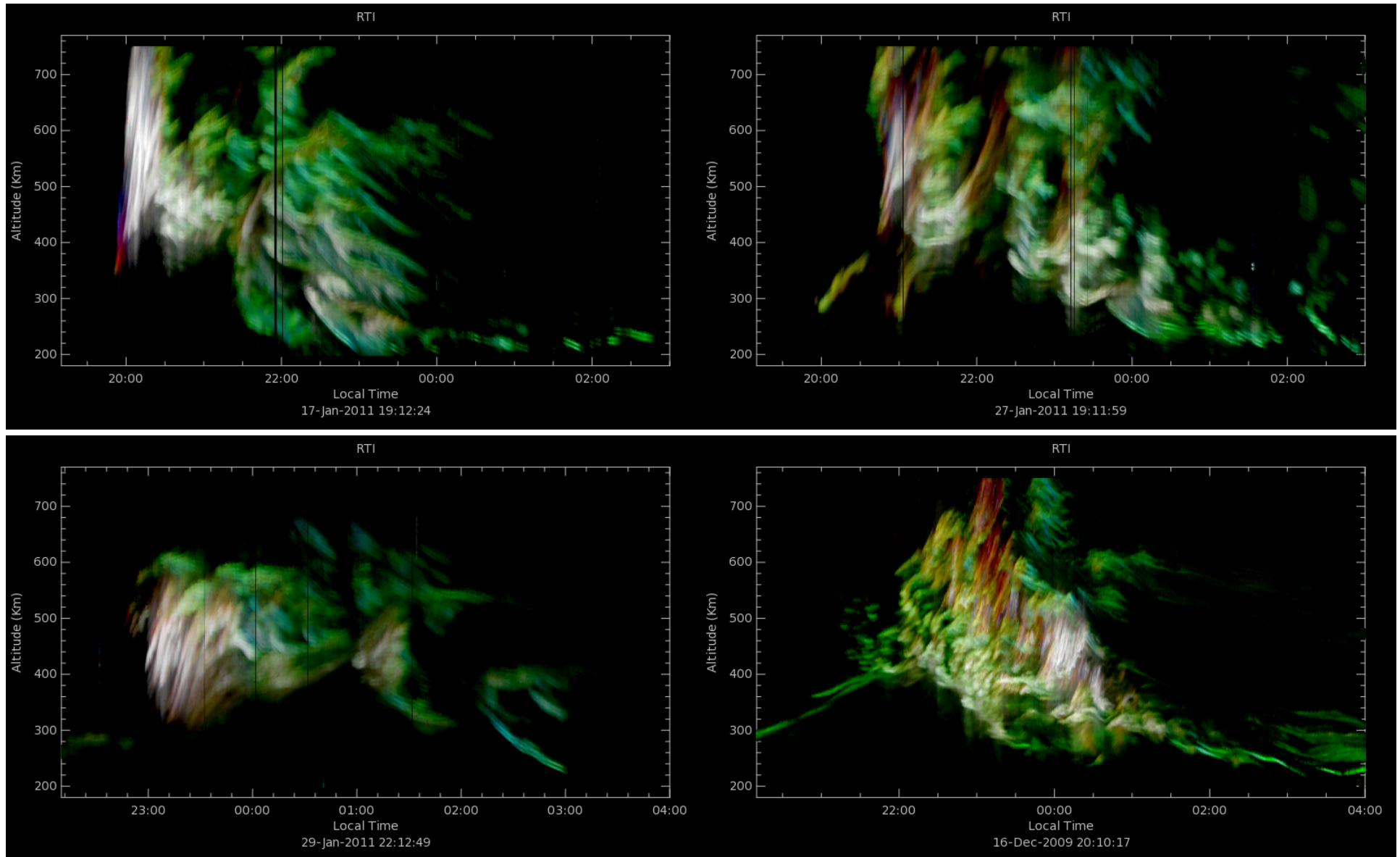
ESF RTDI: Slit camera interpretation

RTDI over JRO ESF (ME)

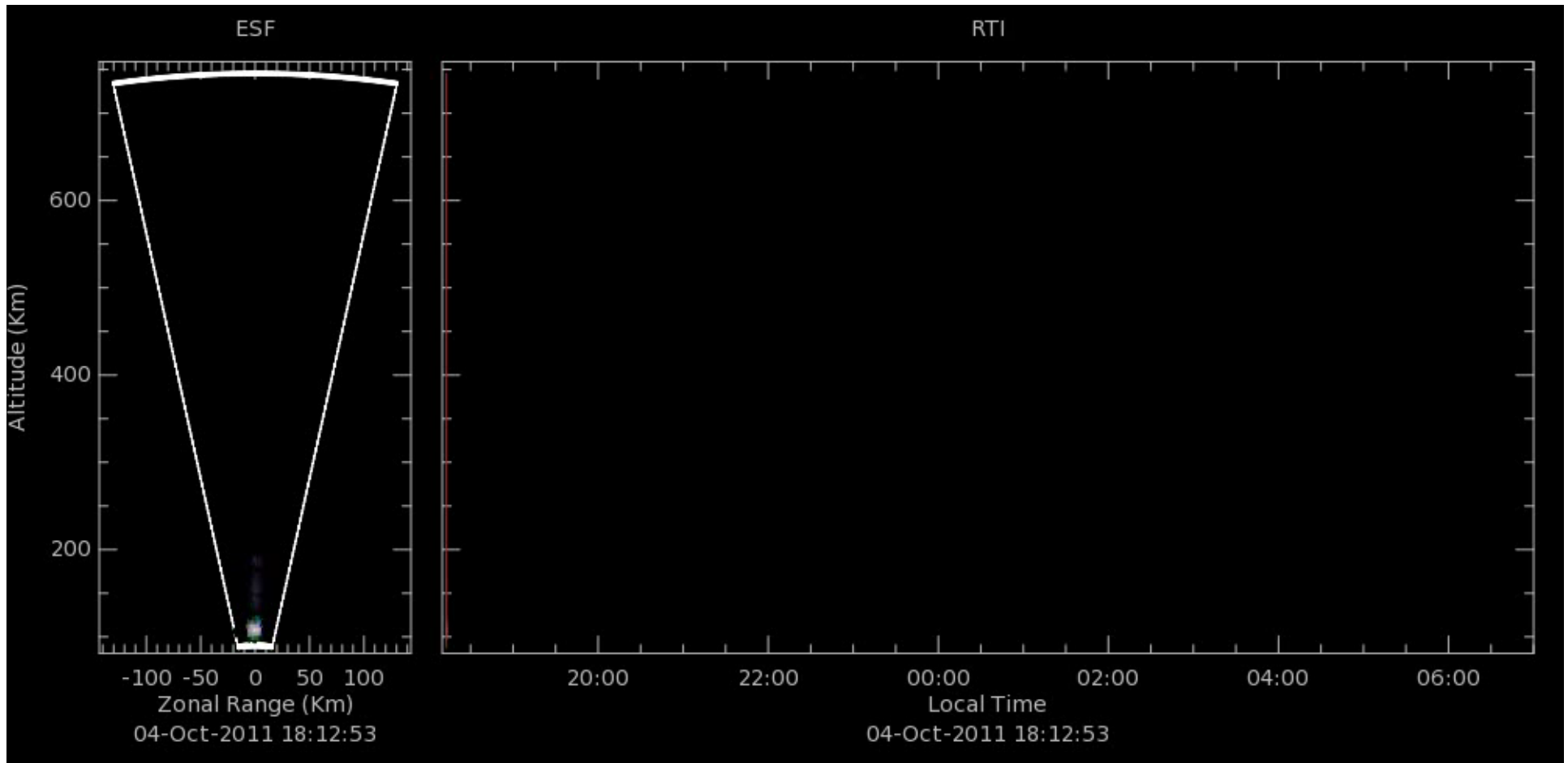


- Typical RTI maps are shown with “false” colors (colors from a pre-defined color table are associated to the signal intensity).
- Here we use Doppler for color. True 24-bit color range time intensity (RTI) plot using Doppler information (RTDI). RTI map is obtained for three Doppler regions centered around: -ve (Red), zero (Green), and +ve (Blue) Doppler velocities.
- It allows, for example, identification of regions and times where there is a depletion channel pinching off, Doppler aliasing, Doppler widening, etc.

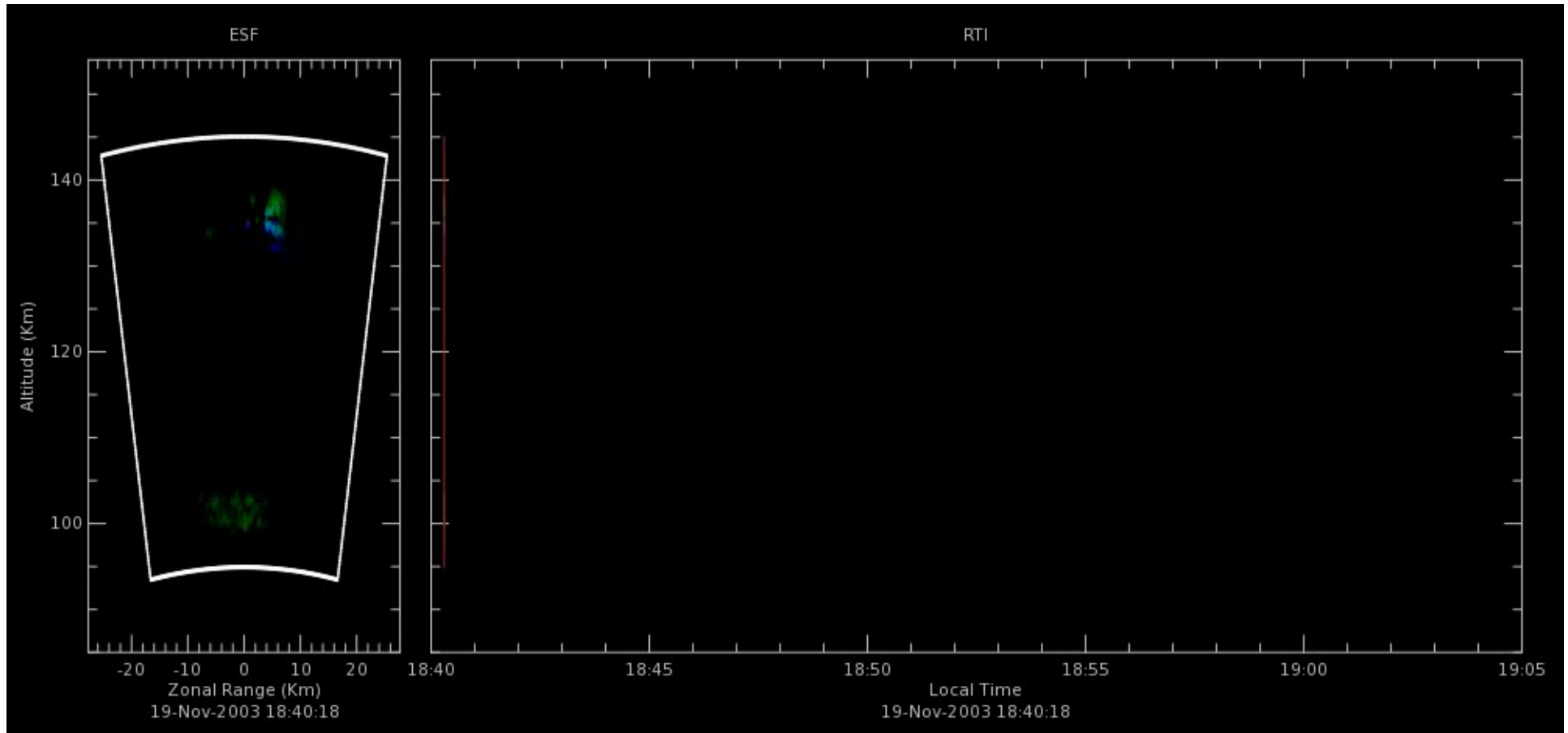
Examples of ESF RTDI



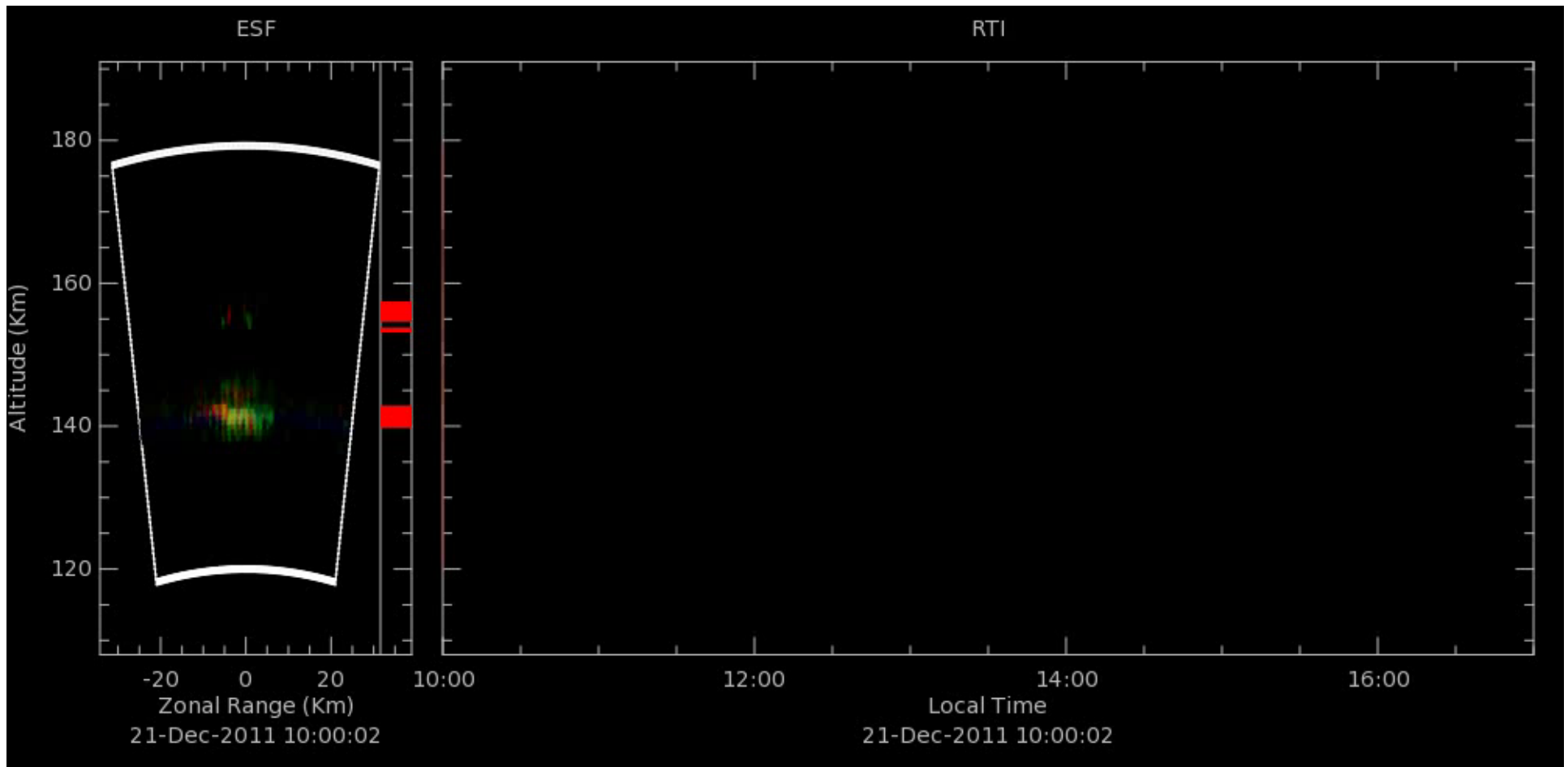
ESF RTDI + Imaging (1)



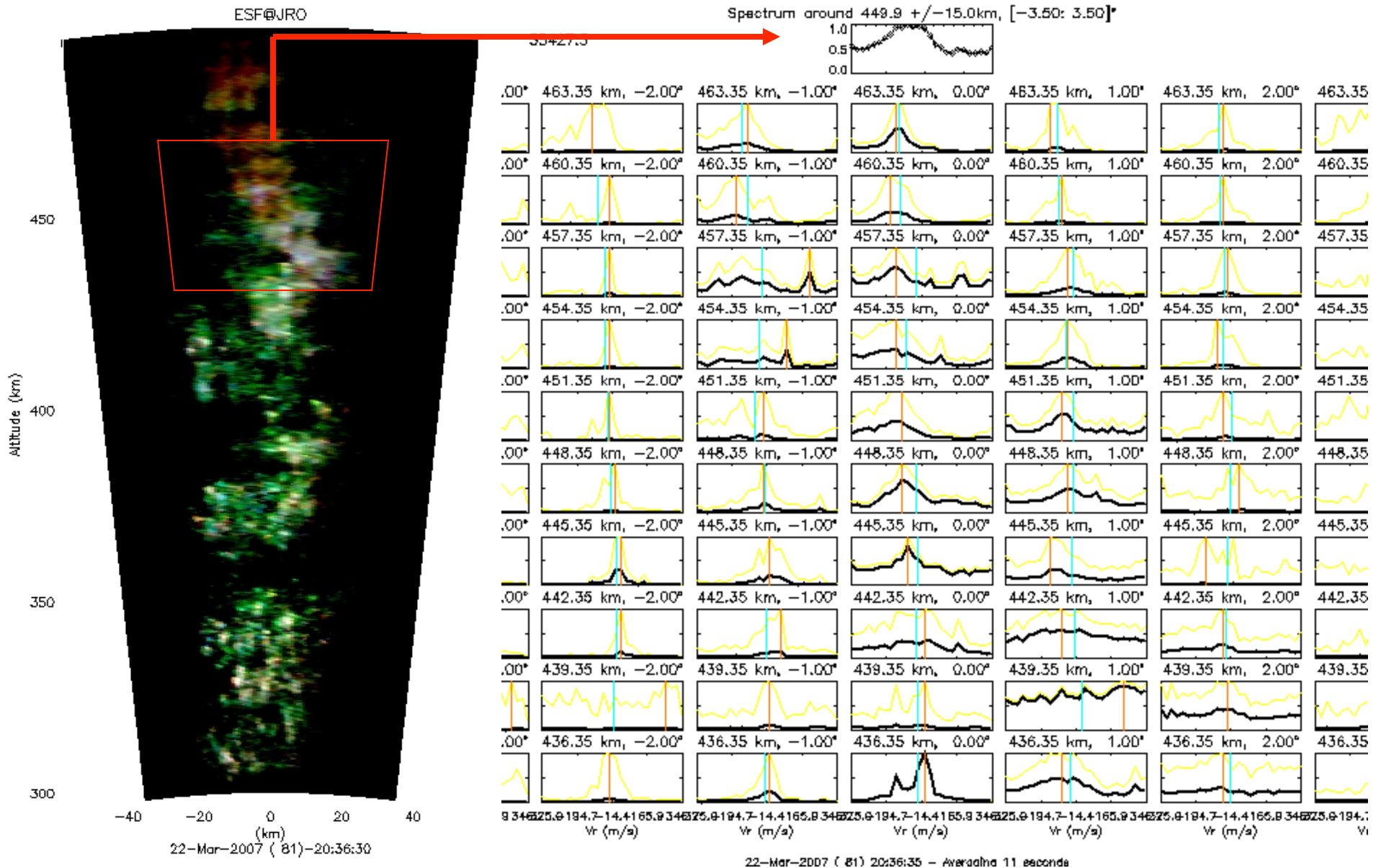
Upper E region RTDI + Imaging



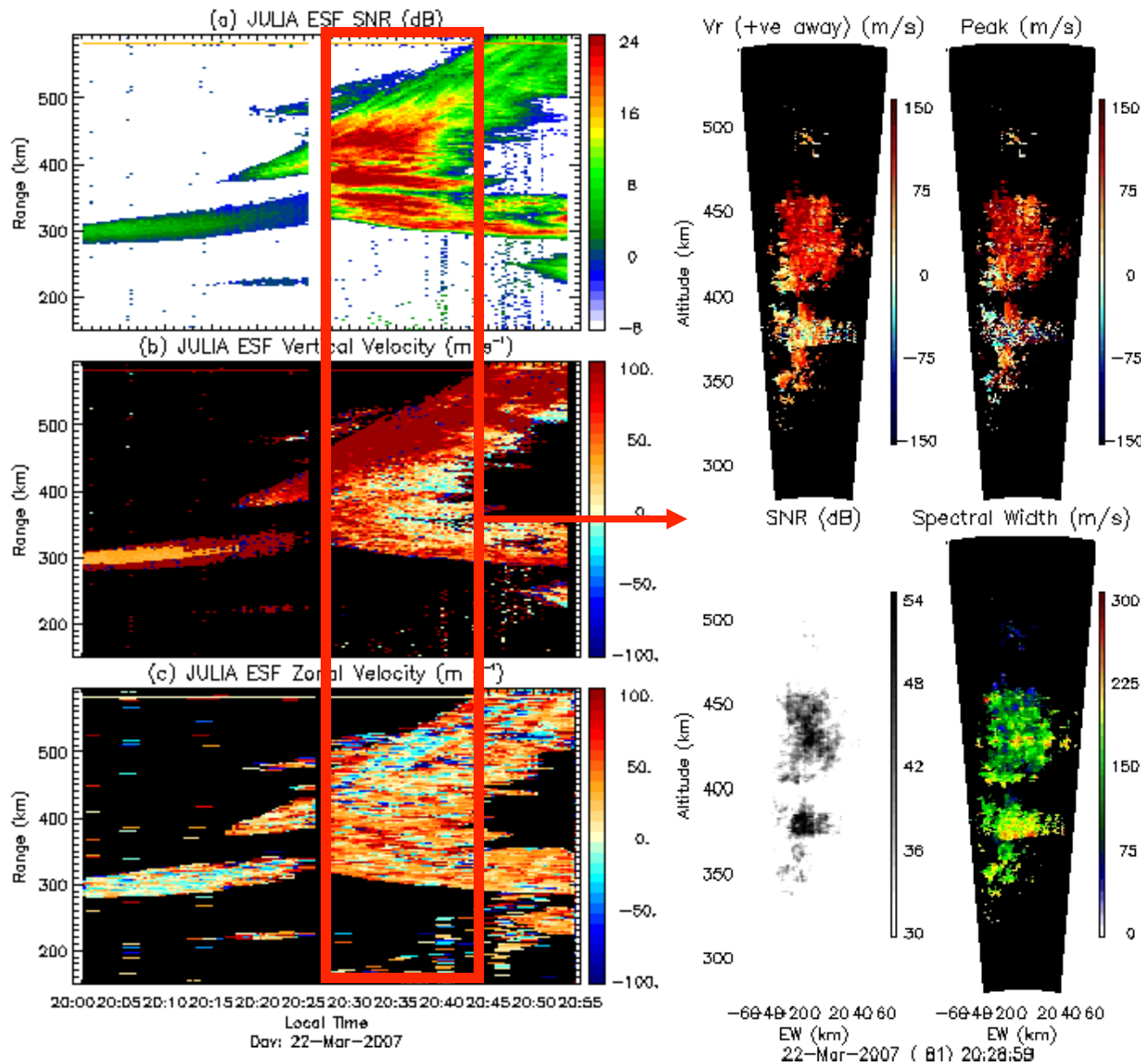
150-km RTDI + Imaging



Spectra cuts from Imaging results

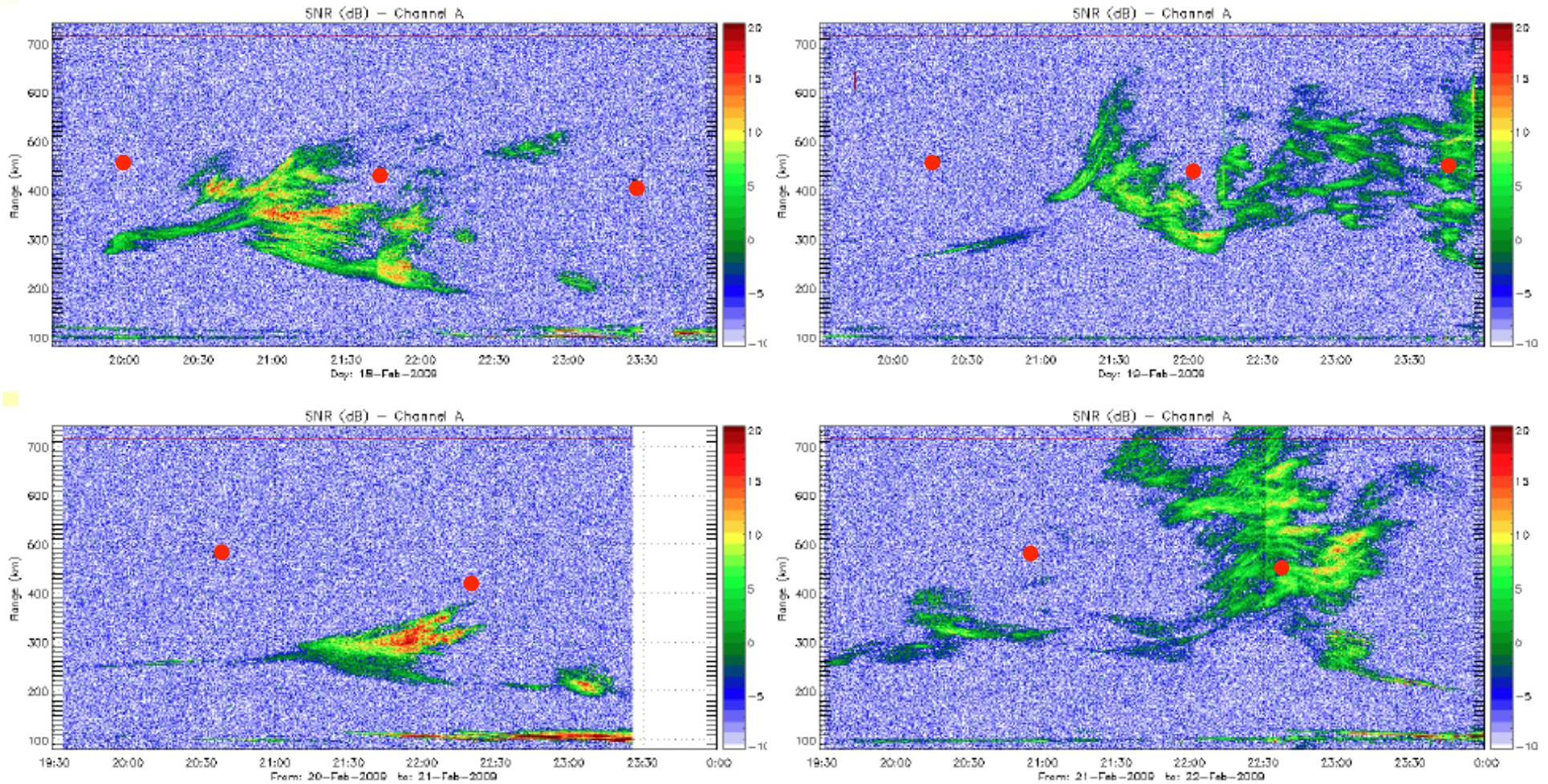


Multi-beam Radar Observations from “Imaging”

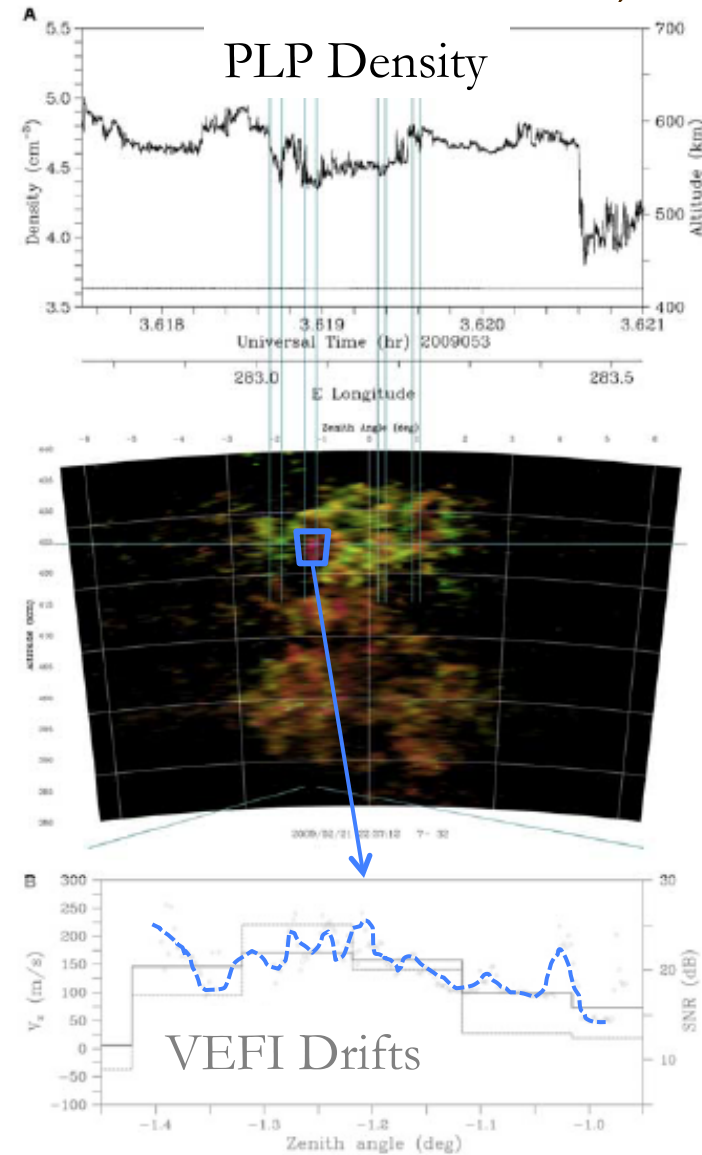
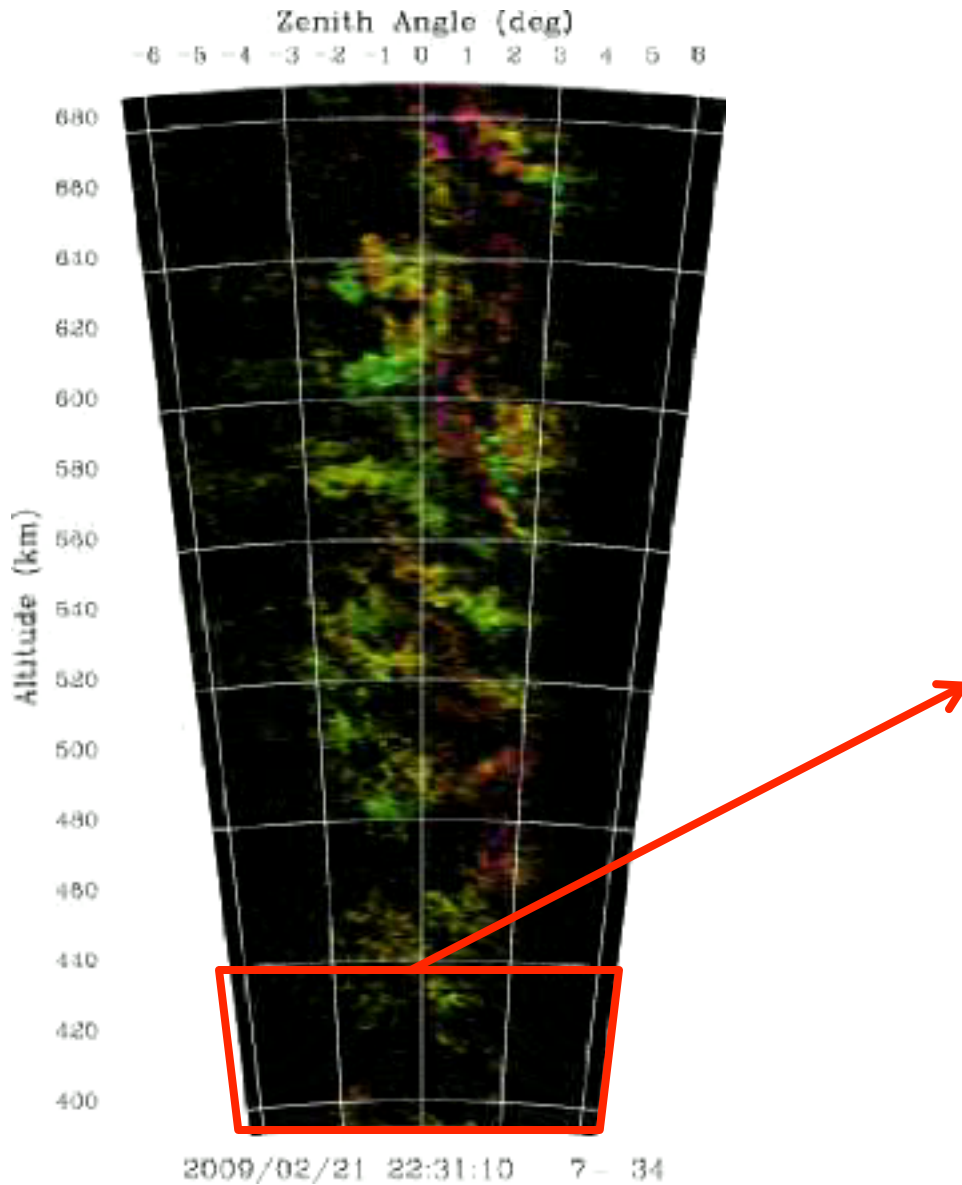


- JULIA-like parameters can be obtained from interferometry using a pair of antennas (SNR, mean vertical Doppler, zonal drift).
- Using imaging, we can get the spectra for different synthesized beams and range resolutions. In this example, each synthesized “scattering volume” is 0.2° and 600m obtained every 10 sec.
- Investigate the possibility of estimating the irregularity spectrum by measuring the radar Doppler spectrum with different averaging volumes [e.g., *Hysell and Chau, 2004*]

Common volume: C/NOFS vs JRO



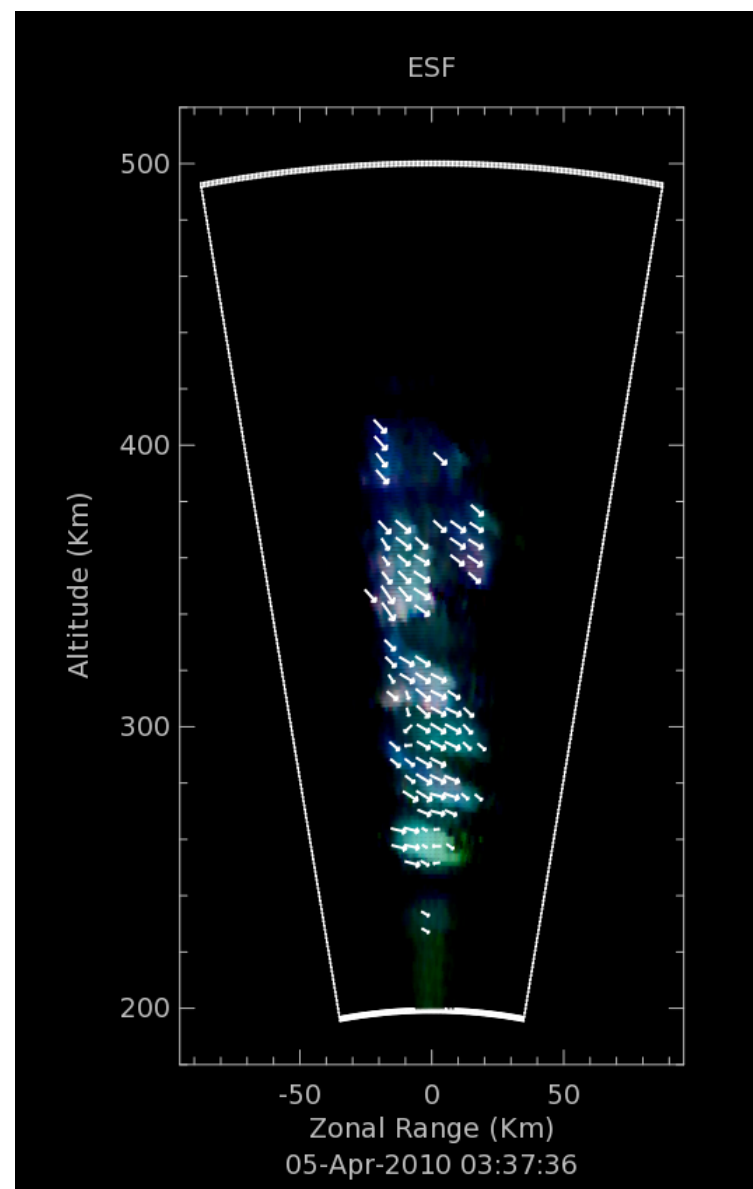
Irregularity comparison: In-situ vs. Radar



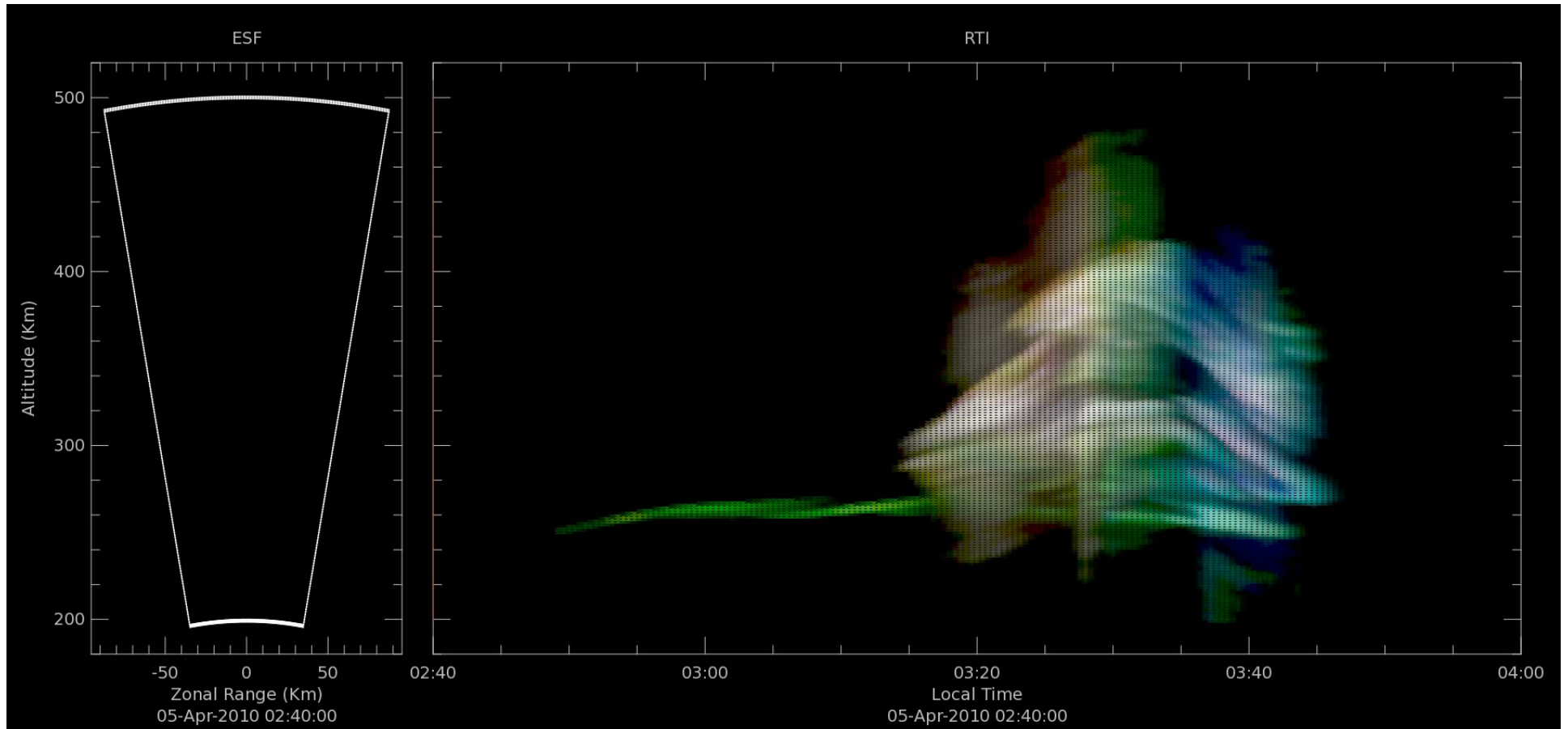
[from *Hysell et al.*, 2009]

Latest developments

- Real time processing
 - Optimized code (memory, loops, ...)
 - Use of Multithreads in an 8-core PC.
 - 10sec, 100-1000 km, 1.5 km res., 16 FFT points, 8 rxs.
- Determination of “blob” vector motion - Particle Image Velocimetry (PIV)



Imaging + PIV



Summary



- Coherent scatter radars should have aperture synthesis radar capabilities to:
 - Resolve space and time ambiguities
 - Increase the angular resolution with small additional modules.
- Nowadays processing can be done in realtime, even when MaxEnt methods are used.
- Robust phase calibration procedures are needed particularly for “real-time” applications.
- In some applications, antenna compression techniques are good complement for aperture synthesis imaging.

Kiitos

Ionospheric Radar Imaging: General Considerations



- In atmospheric/ionospheric radar imaging, scattered signals are caused by **refractive index fluctuations** on the propagation path of transmitted radar pulses.
- **At VHF and higher frequencies** the scattered signal fraction is so minor that there is **no need to consider secondary scattering** of the scattered signals or the extinction of a propagating pulse due to scattered energy.
- From Radio Astronomy jargon, we called:
 - *Brightness*, the angular distribution $[B(\theta_x, \theta_y)]$ of the target we are after (e.g., EEJ, ESF) multiplied by the transmitting and receiving antenna patterns.
 - *Visibility*, the spatial autocorrelation function of the field at the aperture, due to the *Brightness*. It is a function of distance in x and y $[V(r_x, r_y)]$.
- From analogy with temporal-frequency spectral estimation:
 - The **largest separation between antennas**, is equivalent to the observation time. Therefore it **determines the angular resolution**.
 - The **shortest separation** between visibility samples, is equivalent to temporal sampling period, and determines the maximum unambiguous angular range that can be imaged (“**Nyquist**” angle).

PIV – Cross Correlation

